

Published in final edited form as:

Free Radic Biol Med. 2010 April 15; 48(8): 1051–1063. doi:10.1016/j.freeradbiomed.2010.01.021.

The NRF2-heme oxygenase-1 system modulates cyclosporine A-induced epithelial-mesenchymal transition and renal fibrosis

Dong-ha Shin^{1,#}, Hyun-Min Park^{1,#}, Kyeong-Ah Jung¹, Han-Gon Choi¹, Jung-Ae Kim¹, Dae-Duk Kim², Sang Geon Kim², Keon Wook Kang³, Sae Kwang Ku⁴, Thomas W. Kensler⁵, and Mi-Kyoung Kwak^{1,*}

¹Yeungnam University, College of Pharmacy, Gyeongsan-si, Gyeongsangbuk-do 712-749, South Korea

²Seoul National University, College of Pharmacy, Seoul, South Korea

³Chosun University, College of Pharmacy, Gwangju, South Korea

⁴Daegu Hanny University, College of Oriental Medicine, Daegu, South Korea

⁵Johns Hopkins University Bloomberg School of Public Health, Department of Environmental Health Sciences, Baltimore, MD, USA

Abstract

Epithelial-mesenchymal transition (EMT) is an underlying mechanism of tissue fibrosis by generating myofibroblasts, which serve as the primary source of extracellular matrix production from tissue epithelial cells. Recently, it has been suggested that EMT is implicated in immunosuppressive cyclosporine A (CsA)-induced renal fibrosis. In the present study, the potential role of NRF2, which is the master regulator of genes associated with the cellular antioxidant defense system, in CsA-induced EMT-renal fibrosis has been investigated. Pre-treatment of rat tubular epithelial NRK-52E cells with sulforaphane, an activator of NRF2, could prevent EMT gene changes such as the loss of E-cadherin and the increase of α -smooth muscle actin (α -SMA) expression. Conversely, genetic inhibition of NRF2 in these cells aggravated changes in CsA-induced EMT markers. These *in vitro* observations could be confirmed *in vivo*: CsA-treatment developed severe renal damage and fibrosis with increased expression of α -SMA in NRF2-deficient mice compared to wild-type mice. NRF2-mediated amelioration of CsA-EMT changes could be accounted in part by the regulation of heme oxygenase-1 (HO-1). CsA treatment increased HO-1 expression in an NRF2-dependent manner in NRK cells as well as murine fibroblasts. Induction of HO-1 by CsA appears to be advantageous by counteracting EMT gene changes: specific increase of HO-1 expression by cobalt protoporphyrin prevented CsA-mediated α -SMA induction, while genetic inhibition of HO-1 by siRNA substantially enhanced α -SMA induction compared to control cells. Collectively, our current results suggest that the NRF2-HO-1 system plays a protective role against CsA-induced renal fibrosis by modulating EMT gene changes.

© 2010 Elsevier Inc. All rights reserved.

*Corresponding Author: M-K Kwak, Yeungnam University, College of Pharmacy, 214-1 Dae-dong, Gyeongsan-si, Gyeongsangbuk-do 712-749, South Korea. Tel: +82-53-810-2823, Fax: +82-53-810-4654, mkwak@ynu.ac.kr.

#Author contributions: D-H Shin and H-M Park contributed equally to this work.

Publisher's Disclaimer: This is a PDF file of an unedited manuscript that has been accepted for publication. As a service to our customers we are providing this early version of the manuscript. The manuscript will undergo copyediting, typesetting, and review of the resulting proof before it is published in its final citable form. Please note that during the production process errors may be discovered which could affect the content, and all legal disclaimers that apply to the journal pertain.

Keywords

renal fibrosis; cyclosporine A; EMT; NRF2; HO-1; antioxidant defense system; oxidative stress

Introduction

Cyclosporine A (CsA) is the most widely used immunosuppressive drug in organ transplantation and in the therapy of autoimmune disorders. However, nephrotoxicity, which is the frequent side effect of CsA, often hampered the clinical use of CsA [1, 2]. In short-term treatment, CsA induces a reduction of renal blood flow and the glomerular filtration rate, which is attributed to an increase in vasoconstriction factors such as angiotensin II and endothelin. It is believed that a sustained restriction of blood supply in the kidney can cause acute renal dysfunction following CsA treatment. Chronic CsA treatment can lead to an irreversible renal failure with severe tubulointerstitial fibrosis and glomerular sclerosis [2–5]. Involvement of reactive oxygen species (ROS) has been suggested to underlie CsA induced nephrotoxicity. The imbalance of vasoconstriction factors can induce tubular hypoxia-reoxygenation, which in turn increases ROS generation. Indeed, levels of ROS and lipid peroxides were elevated and the cellular GSH pool was decreased following CsA treatment in rat kidneys [6–8].

Epithelial-mesenchymal transition (EMT) is recognized by a loss of epithelial cell phenotype and a concomitant development of mesenchymal phenotype [9–11]. Expression of intercellular epithelial adhesion molecules such as E-cadherin is decreased and markers of mesenchymal cells such as α -smooth muscle actin (α -SMA), N-cadherin and vimentin are induced by EMT. It has been found that the myofibroblast is a key mediator of renal fibrosis and can be generated from epithelial cells. When activated by several growth factors such as transforming growth factor β (TGF β), myofibroblasts function as the primary source for producing extracellular matrix (ECM), including collagen and fibronectin. Therefore, EMT is now accepted as a cellular/molecular mechanism of renal fibrosis [12–14]. A study by Slattery et al., has demonstrated that CsA involves the EMT process in human renal epithelial cells [15].

The cellular defense system against oxidative stress is composed of a subset of genes producing antioxidant proteins, including GSH generating enzymes [e.g., glutamate cysteine ligase (GCL), glutathione reductase], thiol-containing proteins [e.g., thioredoxin, peroxiredoxin], stress-response proteins [e.g., heme oxygenase-1 (HO-1)], and xenobiotic metabolizing enzymes [e.g., glutathione S-transferases (GSTs)] [16–18]. Both basal and inducible expression of many these antioxidant enzymes are regulated by the CNC-bZIP (cap'n'collar family of basic leucine-zipper) transcription factor NRF2 through the antioxidant response element (ARE). Under basal conditions, NRF2 is anchored in the cytoplasm by Kelch-like ECH associated protein 1 (KEAP1), which in turn mediates proteasomal degradation of NRF2 by acting as an adaptor protein of the Cul3-based E3 ubiquitin ligase complex [16, 19]. Mild oxidative and electrophilic stresses disrupt the binding of NRF2 and KEAP1 by modifying several cysteine residues of KEAP1, resulting in accumulation of NRF2 within the nucleus and further transactivation of ARE-bearing genes. Numerous comparative studies of the phenotypes of wild-type and *NRF2*-disrupted mice have revealed the pivotal role of NRF2 in protection against oxidant injuries: *NRF2*-disrupted mice have been much more susceptible to toxicities mediated by environmental chemicals and stresses than wild-type mice [20–23]. It has been well documented that chemicals such as sulforaphane (SFN), dithiolethiones and triterpenoids can efficiently protect normal cells and tissues from oxidant injuries through activation of the NRF2 pathway [22]. One important NRF2-target gene, HO-1, catalyzes heme metabolism, yielding

iron, carbon monoxide and bilirubin. HO-1 is recognized as a protective gene in the kidney involved in degradation of pro-oxidant heme, resulting in production of anti-inflammatory, antioxidant, and anti-apoptotic metabolites [24].

As a consequence, we hypothesized that the NRF2 pathway may modulate the CsA-induced EMT-renal fibrosis by ameliorating CsA-mediated stress, particularly through the induction of HO-1 and other antioxidant genes. Our current study shows that NRF2 activation with SFN could attenuate CsA-induced EMT changes, including the loss of epithelial marker E-cadherin and the acquisition of myofibroblast markers (*e.g.* α -SMA) in normal rat proximal tubule epithelial cells. Involvement of the NRF2 system in CsA-EMT could be confirmed by demonstrating that inhibition of NRF2 in NRK cells facilitated CsA-induced EMT compared to control cells. Regulation of HO-1 could largely account for the protective role of NRF2 in CsA-induced EMT: CsA-mediated α -SMA expression was greatly enhanced by the genetic inhibition of HO-1 expression, while specific induction of HO-1 could prevent CsA-mediated EMT changes. Lastly, in animals, CsA treatment for 2 weeks led to a higher degree of interstitial fibrosis in *NRF2*-deficient mice than in wild-type mice.

Materials and method

Materials

CsA, cobalt protoporphyrin (CoPP), and SFN were purchased from Sigma (Saint Louis, MO, USA). Antibodies recognizing NRF2, lamin B, and β -tubulin were obtained from Santa Cruz Biotechnology (Santa Cruz, CA, USA). E-cadherin antibody was purchased from BD Biosciences (Mississauga, ON, Canada) and α -SMA antibody was obtained from DAKO (Glostrup, Denmark). The reporter plasmid containing the human NQO1 ARE was a gift from Dr. Nobunao Wakabayashi (Johns Hopkins University, MD, USA). Lentiviral plasmid with NRF2 shRNA and the viral packaging mix were purchased from Sigma. Pre-designed HO-1 siRNA and negative control scrambled siRNA (scRNA) were obtained from Bioneer (Daejeon, South Korea). All other reagents were purchased from Sigma

Cell culture

MEF (murine embryonic fibroblasts) from wild-type and *NRF2*-disrupted mice [17] were maintained in Iscoves's Modified Dulbecco's Medium (HyClone, Logan, Utah, USA) containing 10% fetal bovine serum, 4mM L-glutamine, HEPES, and 1% penicillin/streptomycin (HyClone). Normal rat kidney tubular epithelial cells (NRK-52E) were obtained from American Type Culture Collection (Rockville, MD, USA) and were cultured in Dulbecco's Modified Eagle's Medium (HyClone) containing 10% fetal bovine serum, 4 mM L-glutamine, and 1% penicillin/streptomycin.

Cytotoxicity measurement

Cells were plated in 96-well plates and incubated for 24 h. Then, cells were treated with CsA (2, 4 and 8 μ M) for 48 h and then 50 μ l of reagent solution mixed with 0.05 μ l bis-AAF-R110 substrate (Promega) was added to each well. Substrate containing solution was incubated for a further 2 h with orbital shaking at 37°C. Intensities of fluorescence were measured using Fluostar Optima (Offenburg, Germany) at the 485 nm Ex/520 nm Em.

MTT assay

Cells were plated at a density of 5×10^3 cells/well in 96-well plates. After 24 h of incubation cells were treated with CsA. Then, MTT solution (2 mg/ml) was added to each well and cells were further incubated for 4 h. Following the removal of MTT solution 100 μ l of DMSO was added in each well and absorbance was measured at 540 nm using a Versamax microplate reader (Sunnyvale, CA, USA).

Reverse transcriptase-polymerase chain reaction (RT-PCR) and real-time PCR analysis

Total RNAs were isolated from cells using a Trizol reagent (Invitrogen, Carlsbad, CA, USA) following treatment of cells with CsA. For the synthesis of cDNAs, reverse transcriptase reaction was performed by incubating 200 ng of total RNA with a reaction mixture containing 0.5 $\mu\text{g}/\mu\text{l}$ oligo dT₁₂₋₁₈, 200 U/ μl Moloney Murine Leukemia Virus reverse transcriptase (Invitrogen) and Fail Safe master buffer (Epicentre, Madison, WI, USA). PCR amplification for each gene was carried out with a thermal cycler (Bio-Rad, Hercules, CA, USA) and amplification conditions were 27–30 cycles of 40 s at 95°C, 30 s at 56°C and 30 s at 72°C. For the real-time PCR analysis, Roche LightCycler (Mannheim, Germany) was used with Takara SYBR Premix ExTaq system (Otsu, Japan). Primers were synthesized by Bioneer (Daejeon, South Korea) and primer sequences for rat genes are: rat E-cadherin, 5'-AGAAGAAGACCAGGACTTTG-3' and 5'-CGTTCAGATAATCGTAGTCC-3'; rat Fn-1, 5'-TATGCTCTCAAGGACACATT-3' and 5'-TATGCTCTCAAGGACACATT-3'; rat vimentin, 5'-AGCAGGAGTCAAACGAATAC-3' and 5'-GGTTAGTTTCTCTCAGGTTC-3'; rat α -SMA, 5'-CGACATGGAAAAGATCTGGC-3' and 5'-GGATCTTCATGAGGTAGTCG-3'; rat HPRT, 5'-ATCAGACTGAAGAGCTACTG-3' and 5'-GCTGATGACACAAACATGAT-3'; rat HO-1, 5'-CACCAAGTTCAAACAGCTCT-3' and 5'-CAGGAAACTGAGTGTGAGGA-3'; rat NQO1, 5'-TCCATGTACTCTCTGCAGG-3' and 5'-TTCTAGCTTTGATCTGGTTG-3'; rat catalytic subunit of GCL (GCLC), 5'-GACCAATGGAGGTACAGTTG-3' and 5'-CCATGTTTTCAAGGTAGGAG-3'; rat modulatory subunit of GCL (GCLM), 5'-CTTTCCTGGAGCATTGCA-3' and 5'-TGATTCCTCTGCTTTTCACG-3'; mouse TGF β , 5'-ACTCCACGTGGAAATCAACG-3' and 5'-TCCAGGCTCCAAATATAGGG-3'; mouse α -SMA, 5'-AGCTGTGCTATGTAGCTCTG-3' and 5'-TCTGCATCCTGTCAGCAATG-3'; mouse HPRT, 5'-AGATCTCATGAAGGAGATGG-3' and 5'-TACAGTAGCTCTTCAGTCTG-3'. PCR products were resolved on 1.2% agarose gels and the images were captured by using a Visi Doc-It™ Imaging system (UVP, Upland, CA, USA). Intensities of each blot were quantified by using the Image J software (National Institute of Mental Health, Bethesda, MD, USA).

Preparation of nuclear extracts

Nuclear proteins from NRK cells were extracted as described previously. Briefly, crude nuclear fractions were obtained by lysing cells with homogenization buffer (2 M sucrose, 1 M HEPES, 2 M MgCl₂, 2 M KCl, 30% glycerol, 0.5 M EDTA, 1 M DTT, protease inhibitor cocktail (Sigma), and 0.2% NP40) and followed by centrifugation at 12,000 *g* for 15 min. Nuclear proteins were extracted from obtained crude nuclear fractions by incubating with extraction buffer containing 20 mM HEPES (pH 7.9), 1.5 mM MgCl₂, 420 mM NaCl, 10% glycerol, 0.2 mM EDTA and protease inhibitor cocktail for 30 min on ice. Protein concentration was determined by the RC DC protein assay kit (Bio-Rad).

Immunoblot analysis

Cell lysates were loaded on 6% or 12% SDS-polyacrylamide gels and separated by electrophoresis. Proteins on gels were transferred to nitrocellulose membrane (Whatman, Dassel, Germany) and membranes were blocked with 5% skim milk in TPBS buffer (8 g/l NaCl, 0.2 g/l KCl, 1.44 g/l Na₂HPO₄, 0.24 g/l KH₂PO₄ and Tween-20 2 ml/l) for 1 h. Then, primary antibody incubation was performed for overnight and followed by incubation with secondary antibody conjugated with horseradish peroxidase (Bio-Rad) for 1 h. Detection was done with the Enhanced Chemiluminescence reagent (Amersham Biosciences, Buckinghamshire, UK).

Immunocytochemistry

NRK-52E cells were grown on chamber slides (Nalgene Nunc International, Rochester, NY, USA) at a density of 5×10^4 cells per well. After 24 h, cells were pre-treated with vehicle (dimethylsulfoxide, DMSO) or SFN (1.25 μ M) for 24 h and vehicle (Veh, ethanol) or CsA (8 μ M) was incubated for 48 h. Cells were washed with PBS, fixed by 4% paraformaldehyde for 20 min and permeabilized with 0.1% Triton X-100 for 10 min at room temperature. Then cells were blocked by Image-iT™ FX signal Enhancer (Molecular probes, Eugene, Oregon, USA) for 30 min at room temperature and anti-E-cadherin antibody (1:100 dilution) or anti- α -SMA antibody (1:100 dilution) was incubated for 1.5 h at room temperature. Then, the reaction of cells with Alexa Fluor® 488 conjugated donkey anti-mouse IgG (10 μ g/ml, Molecular probes) for 1.5 h was followed by incubation with DAPI (300 nM, Molecular probes) for 10 min. Then images were visualized with a fluorescence microscope (Eclipse TE2000-U, Nikon, Melville, USA)

Reporter plasmid transfection and luciferase activity measurement

Cells were transfected with plasmids at 50% confluence by using Welfect-Ex™ Plus Transfection Reagent (WelGene Inc., Daegu, South Korea). Briefly, cells were incubated with the transfection complex containing 0.5 μ g ARE-luciferase plasmid, 0.05 μ g pRLtk control plasmid and the transfection reagent (Welfect-Ex™ 2 μ g and Enhancer-Q™ 1.5 μ g) in serum- and antibiotic-free OptiMEM medium (Invitrogen). Transfection was continued for 18 h; cells then recovered in the complete medium for the next 24 h and were lysed. Then, luciferase activities from Firefly and Renilla luciferases in total cell lysates were determined using a Dual-Luciferase Assay kit (Promega) with a 20/20ⁿ luminometer (Turner Biosystems, CA, USA).

Measurement of total GSH and GSSG contents

Cells were grown in 96-well plates for 24 h and lysed with 30 μ l of 5% metaphosphoric acid solution. For the measurement of total GSH content, optical densities were monitored for 4 min following the addition of 30 μ l 5',5-dithiobis (2-nitrobenzoic acid), GR and β -NADPH [25]. For the measurement of oxidized GSH (GSSG), 2-vinylpyridine (10 μ M) was added into cell lysates and assay was performed following incubation for 1 h. Protein concentration was determined by BCA™ protein assay kit (Pierce, Rockford, IL, USA).

Production of lentiviral particles with NRF2 shRNA expression vector

Lentiviral particles with shRNA were produced in HEK 293T cells following transfection with NRF2 shRNA expression plasmid (Sigma) and Mission™ Lentiviral Packaging Mix (Sigma). Briefly, HEK 293T cells were seeded on 60 mm plates at a density of 7×10^5 cells per well. The next day, medium was replaced by OptiMEM in the absence of antibiotics and subsequently 1.5 μ g pLKO.1-NRF2 shRNA, which contains human NRF2-specific shRNA (5'-CCGGGCTCCTACTGTGATGTG-AAATCTCGAGATTTACATCACAGTAGGA-3'), and the Packaging Mix were transfected into cells by using Lipofectamine™ 2000 (Invitrogen) according to the manufacturer's instruction [26]. pLKO.1-scrRNA plasmid was used as a nonspecific control RNA. On the second day, media with transfection complex were removed and the complete medium was added into each well. On the third and fourth days, media containing lentiviral particles were harvested and collected viral particles were stored at -70°C .

Establishment of NRF2-knockdown NRK cells

NRK cells were seeded on 6-well plates at a density of 2×10^5 cells per well and were transduced with lentiviral particles containing either non-specific scrRNA expression plasmid or NRF2 shRNA expression plasmid in the presence of 8 μ g/ml of hexadimethrine bromide

(Sigma). Transduction was continued for 24 h followed by a 48 h recovery in the complete medium. For the selection of cells with target plasmids, cells were transferred into 96-well plates at a density of 100 cells per well and were grown in a medium with 1 $\mu\text{g/ml}$ puromycin (Sigma). Isolated individual colonies were kept for up to 3 weeks and inhibition of NRF2 was verified in each colony by measuring NRF2 and its target genes.

HO-1 or scrambled siRNA transfection

Pre-designed and pre-annealed HO-1 siRNA (5'-ACAAGCAGAACCCAGUCUA-3' and 5'-UAGACUGGGUUCUGCUUGU-3') was obtained from Bioneer. Negative control siRNA comprised of a 19 bp scrambled sequence with 3' dT overhangs that was also purchased from Bioneer. Cells were seeded in 6-well plates at a density of 1.5×10^4 cells and grown for 24 h in the absence of antibiotics. Transfection was performed with Lipofectamine™2000 reagents. Briefly, appropriate amount of siRNAs in 250 μl Opti-MEM I medium and pre-diluted 5 μl lipofectamine solution were combined and further incubated for 20 min. Transfection mixture was added into each well and incubated for 96 h in Opti-MEM reduced serum medium.

Animal treatment

Male mice (ICR, 9-week old) with either *NRF2* +/+ or *NRF2* -/- genotype [27] were fed with 0.01% low sodium AIN-76A purified diets (Feed Lab, Gyeonggi-do, South Korea) for a week before starting and during CsA treatment. Mice were treated with either olive oil (5 ml/kg) or olive oil-suspended CsA (30 mg/kg) by *gavage* for 2 weeks. Mice were sacrificed and samples (blood and kidneys) were collected for measurement of renal function and RNA extraction. For HO-1 mRNA measurement, wild-type ICR mice were treated with CsA for two consecutive days and RNA analysis was carried out in the kidneys. Animal protocols were approved by the Johns Hopkins Animal Care and Use Committee.

Measurement of renal function

Renal injury was monitored by measuring levels of serum creatinine levels. Blood was collected from vehicle (olive oil) or CsA-treated mice from the vena cava. Obtained blood was kept at room temperature for coagulation and centrifuged at $6,000 \times g$ for 20 min for serum preparation. Then, DICT-500 (BioAssay Systems, Hayward, CA, USA) was added into serum samples and optical density values of creatinine were measured at 510 nm using a Versamax Microplate Reader.

Histology and histomorphometry evaluation

Kidneys were fixed in 10% neutral buffered formalin and a paraffin embedding was carried out. Tissue sections with 3–4 μm thickness were stained with Hematoxylin and Eosin for microscopic evaluation. Percentage of degenerative regions of kidney parenchyma (%/mm² of kidney parenchyma) and abnormal tubule numbers among 1,000 observed tubules were measured using a digital image analyzer (DMI-300, DMI, South Korea). Collagen deposits have been determined by the development of deep green colors following Masson's trichrome staining of tissue sections. Histomorphometrical analysis was conducted in 1 mm² of prepared specimens [28]. Two fields were selected in one kidney sample and, in each group, three kidneys from individual animals were used for this analysis.

Statistical Analyses

Statistical significance was determined by Student paired *t*-test or one-way ANOVA followed by Student-Newman-Keuls's comparison method (SigmaStat analysis software, USA).

Results

CsA induced EMT marker changes in normal rat renal tubular epithelial cells

It has been demonstrated that CsA treatment resulted in morphologic changes, including cell elongation and junctional disruption with an increased expression of myofibroblast-specific marker α -SMA in human proximal tubular cells [15, 29]. This supports the possibility that EMT plays a role in CsA-induced tubulointerstitial fibrosis. Therefore, we have examined the effect of CsA on EMT marker changes in rat renal tubular epithelial NRK cells. As EMT markers, expression of epithelial adhesion molecule E-cadherin was significantly reduced following 8 μ M CsA incubation for 48 h (Fig. 1A). Expression of myofibroblast marker α -SMA and vimentin were increased 3-fold at 8 μ M CsA compared to vehicle control. In addition, transcript level for ECM protein Fn-1 was increased 2.5-fold following CsA incubation for 48 h. However, there was no alteration in TGF β expression following CsA. Changes in EMT marker expression could be observed in lower concentration of CsA, which is more relevant to the plasma concentration of CsA in clinical applications. As shown in Fig. 2B, expression of α -SMA increased by two-fold following incubation with 1 μ M CsA in NRK cells. While, expression of Fn-1 was not elevated at this concentration (Fig. 2B). These results indicate that α -SMA induction is the most initial event occurring at low concentration of CsA, and relatively high concentration of CsA is required for the changes in wide array EMT markers. Alterations in EMT marker expression such as E-cadherin reduction and α -SMA increase were also observed in CsA-incubated cells for 24 h (Fig. 1C). However, there was no alteration in the expression of other markers such as vimentin (Data not shown). In addition to alterations in the expression of EMT markers, CsA induced some morphological changes in NRK cells (Fig. 1D). At the concentrations of 4 and 8 μ M CsA, most of cells lost the contact with neighboring cells and the gaps between cells became wide. Although cell elongation, which is the typical characteristics of mesenchymal cells, has not been observed in these cells, the junctional disruption may indicate epithelial properties were lost by CsA. These results suggest that relatively high concentration of CsA (8 μ M) and 48 h incubation time can be used for the further study on the role of NRF2 in CsA-EMT although some growth inhibition (70–80%) can be found at this treatment schedule (Data not shown). However, when the cytotoxicity was assessed in NRK cells, CsA treatment did not cause a significant cell death up to 8 μ M (Fig. 1E). Collectively, these results indicate that CsA can effectively alter the expression of EMT-associated genes in rat kidney epithelial NRK cells.

SFN increased NRF2 activity and induced NRF2-target gene expression in NRK cells

SFN activates the NRF2 pathway, leading to a coordinated induction of its downstream target genes in many types of cells and tissues. Thus, we investigated whether SFN treatment effectively activates NRF2 in NRK cells. Transcript levels of NRF2-target genes, which have been measured by real-time PCR analysis, showed that NQO1 and GSH-synthesizing GCL subunits were increased following incubation with 1.25 μ M SFN for 24 h (Fig. 2A). The level of HO-1 transcripts was found to increase maximally at 6 h after SFN treatment (Fig. 2A) and only showed a marginal increase 24 h after treatment (Data not shown). In accord with the effects on expression of target genes, SFN increased nuclear levels of NRF2 (Fig. 2B) and the luciferase activities derived from the NQO1 ARE were elevated 3.5-fold by SFN (Fig. 2C). These results collectively support that SFN can effectively activate the NRF2 system in rat kidney epithelial NRK cells.

NRF2 activating SFN could attenuate CsA-induced EMT gene changes in NRK cells

Next, in an attempt to elucidate the potential role of NRF2 activators as modulators of CsA-induced EMT changes, SFN was incubated in NRK cells for 24 h prior to CsA treatment and transcript levels for α -SMA and Fn-1 were determined. At the same time, the effect of the

GSH precursor NAC was examined. Pre-treatment with 1.25 μ M SFN significantly blocked CsA (8 μ M)-induced increase in α -SMA and Fn-1 expression (Fig. 3A), while treatment of cells with NAC did not. Similarly, SFN treatment prevented α -SMA elevation, which was led by 2 μ M CsA (Fig. 3B). In accord with transcript levels, elevation of α -SMA and Fn-1 proteins was effectively suppressed by SFN treatment (Fig. 3C). Reduction in the epithelial marker E-cadherin by CsA was prevented by SFN, while NAC did not show significant alterations in CsA-induced gene expression, a result consistent with the RT-PCR analysis. Similarly, treatment with D3T, another type of NRF2 activator, showed a reduction in CsA-induced EMT marker changes, although the potency is lower than SFN (Fig. 3A). Next, in order to confirm the effect of SFN on CsA-induced EMT gene expression, an immunocytochemical analysis was conducted. Incubation of NRK cells with CsA for 48 h substantively increased α -SMA-positive staining; pre-incubation with SFN for 24 h before CsA blocked this increase (Fig. 3D). E-cadherin-positive staining was observed in cell membranes of control cells and the staining was decreased in CsA-treated cells. Similar to the immunoblot analysis, SFN-treated cells did not exhibit the loss of E-cadherin expression. Taken together, our results support the initial hypothesis that the NRF2 activator SFN can prevent CsA-induced changes in EMT markers in rat renal epithelial cells. However, SFN pre-treatment could not prevent CsA-mediated cell number reduction (Fig. 3E). These results suggest that NRF2 activating SFN can effectively prevent EMT gene changes in rat renal epithelial cells.

NRF2 inhibition in NRK cells exacerbated CsA-induced EMT changes in NRK cell

Our study showed that SFN could prevent EMT gene changes in rat tubular kidney cells, implying that the NRF2-antioxidant system might contribute directly to prevent the CsA-EMT process. In order to confirm this hypothesis, as a loss of function study, NRF2-inhibited NRK cells were established and the effect of CsA was investigated. Lentiviral particles containing the plasmid, expressing either NRF2-specific shRNA or nonspecific scrambled RNA (scRNA), were produced in HEK293T cells and were stably transduced into NRK cells for 4 weeks. Stable cell colonies expressing scRNA (NRK-scRNA) or NRF2 shRNA (NRK-shNRF2) were isolated and NRF2 inhibition and its target gene expression verified. NRK-shNRF2 cells showed 70–80% inhibition in NRF2 transcripts compared to scrambled control cells and in turn the expression of NQO1 and HO-1 was reduced in NRK-shNRF2 cells (Fig. 4A). Thereafter, CsA was incubated for 48 h in both cell lines and transcript levels for EMT makers including α -SMA and Fn-1 were assessed. Induction folds of α -SMA and Fn-1 were significantly higher in NRF2 inhibited cells than in control cells: α -SMA transcripts increased 4-fold and 8-fold in scrambled control RNA and NRF2-shRNA expressing cells, respectively (Fig. 4B and 4D). In accord with mRNA level changes, induction level of α -SMA protein was greater in NRF2-inhibited cells than that in control cells (Fig. 4C and 4D). These results suggest that inhibition of NRF2 signaling can facilitate CsA-mediated EMT changes in NRK cells.

CsA treatment increased HO-1 expression

Several reports demonstrated that CsA induces ROS generation by altering expression of antioxidant genes. As our results indicate that NRF2 levels can determine the degree of EMT changes in CsA-treated renal epithelial cells, effect of CsA on the antioxidant system could be envisioned. In order to test this possibility, levels of cellular total GSH and oxidized GSSG, and expression of GSH synthesizing enzymes have been asked. CsA treatment did not alter the level of total GSH when compared to vehicle control. In addition, CsA treatment did not change level of oxidized GSH (GSSG) and transcript level for the catalytic subunit of GCL (GCLC) (Fig. 5A and 5B). While, level for the modulatory subunit of GCL (GCLM) was slightly increased by CsA treatment (Fig. 5B). These results indicate that CsA treatment in our system does not lead to the reduction of GSH and the suppression

of its synthesizing enzyme levels, which has been shown in other studies. Whilst, it was notable that the expression of HO-1 was highly induced more following CsA treatment when compared to vehicle control (Fig. 5B). Cells pre-treated with SFN prior to CsA showed a further increase in HO-1 expression, which is accompanied by a reduction of α -SMA expression (Fig. 5E). HO-1 expression is known to be regulated by NRF2 primarily. Next, we investigated whether CsA can increase NRF2 activity in NRK cells. When NRF2 activity was monitored, CsA treatment showed a marginal increase in nuclear level of NRF2 (Fig. 5C); however no significant increase was found in ARE-luciferase activity (Fig. 5D), which indicates that CsA can lead to nuclear accumulation of NRF2 not accompanying the elevation of a broad-ranged increase in its target gene expression. These results show that cellular level of GSH-related gene expression, as well as total GSH content, is not significantly altered by CsA treatment in NRK cells. Together with the previous observation that NAC could not rescue CsA-induced changes in EMT gene expression, it can be concluded that GSH depletion and consequent oxidative stress might not be contributing to the EMT changes induced by CsA in NRK cells.

CsA-induced HO-1 expression was NRF2-dependent and expression level of HO-1 is strongly associated with CsA-mediated α -SMA expression

In our study, inhibition of the NRF2 pathway could enhance CsA-mediated EMT changes, while pharmacological induction of the NRF2 system could attenuate them in rat tubular epithelial cells. In particular, it was notable that CsA can increase the expression of HO-1, which has been known to contribute to the protection of renal tissue from chemical toxicities and fibrosis. Therefore, it can be hypothesized that induction of HO-1 by CsA treatment might be the defense mechanism counteracting CsA toxicity. In order to explore this possibility, we measured levels of HO-1 mRNA following treatment with CsA in NRF2-inhibited NRK cells. Induction fold of HO-1 transcripts by CsA was much lower in NRF2-shRNA cells than that in control cells: HO-1 levels increased by 3.5-fold and 1.5-fold at 7 h after CsA treatment in scRNA (NRK-scRNA) and NRF2 shRNA expressing NRK cells (NRK-shNRF2), respectively (Fig. 6A). NRF2-dependent induction of HO-1 by CsA could be clearly confirmed by results obtained from murine embryonic fibroblasts (MEF) with *NRF2*^{-/-} genotype. When wild-type MEF cells (*NRF2*^{+/+}) were incubated with CsA for 7 h, HO-1 levels were increased about 2-fold, while no increase was observed in *NRF2*-deficient MEFs (Fig. 6B). These results suggest that NRF2-dependent HO-1 expression could be a major contributor to protecting against the CsA-EMT process. Next, in an attempt to clarify the role of HO-1 in CsA-induced EMT changes, specific modulation of HO-1 level was performed by incubating cells with HO-1 inducer CoPP or by introducing HO-1 siRNA. First, when 100 μ M CoPP was pre-incubated for 24 h prior to CsA treatment, HO-1 transcripts were highly elevated and CsA-mediated α -SMA induction was completely blocked by CoPP (Fig. 6C). Second, when NRK cells were transiently transfected with HO-1 targeting siRNA, CsA-mediated α -SMA induction was markedly increased compared to scRNA- and HO-1 specific siRNA-transfected cells, respectively (Fig. 6D). These results support the possibility that HO-1 induction plays an important protective role in the CsA-mediated EMT-renal fibrosis model in an NRF2-dependent manner.

NRF2 knockout mice are much susceptible to CsA-mediated interstitial fibrosis than wild-type mice

Next, in order to clarify the role of NRF2 in CsA-mediated EMT-renal fibrosis pathology, wild-type (*NRF2*^{+/+}) and *NRF2*-deficient mice (*NRF2*^{-/-}) were treated with CsA and changes in α -SMA expression as well as fibrosis makers examined in the kidney. Vehicle (olive oil) or CsA (30 mg/kg, *p.o.*) was administered into mice once a day for 2 weeks and blood and kidneys were collected for the analyses of renal function, RNA, and histological

changes. First, the two-week schedule of CsA treatment did not alter a blood marker of renal dysfunction: serum creatinine levels were not increased in CsA treated mice of either genotype (Fig. 7B). Second, although renal dysfunction was not observed, induction levels of genes, which are associated with EMT, were higher in CsA-treated *NRF2*-disrupted mice than in wild-type mice. Renal transcript level of α -SMA was elevated 1.8-fold by CsA in *NRF2*-disrupted mice but not in wild-type mice (Fig. 7C). In addition, an increase in TGF β expression by CsA treatment was significantly higher in *NRF2*-deficient mice (2.4-fold) than in wild-type mice (1.7-fold). Levels for renal HO-1 expression in CsA-treated wild-type mice were similar to that in vehicle-treated mice (data not shown). However, when wild-type ICR mice were treated with CsA for two consecutive days, HO-1 mRNA level increased by twofold compared to vehicle control (Fig. 7A). These results imply that HO-1 induction in the early phase of CsA treatment could be critical for the renal protection from fibrosis. These results clearly support that our observations *in vitro* studies, which show the inhibitory role of HO-1 in CsA-EMT, could be relevant to CsA-renal fibrosis in animals. Third, when histological changes were examined in the kidneys from CsA-treated mice, CsA toxicity was relatively severe in *NRF2*-disrupted mice compared to that in wild-type mice. Treatment of mice with CsA for 2 weeks induced renal damage in both genotype groups, including epithelial necrosis, tubular damages, and deposition of collagen fibers (Fig. 8A). A histomorphometrical analysis showed that CsA-mediated renal damage was significantly higher in the *NRF2*^{-/-} mice with regard to the increase in percentage of degenerative regions (Fig. 8A) and numbers of abnormal tubules (data not shown). Furthermore, staining of tissue collagen with Masson's trichrome could demonstrate that percentage of collagen fiber deposited regions in the kidney was significantly higher in CsA-treated *NRF2*^{-/-} mice: 35% collagen deposited regions have been observed in *NRF2*-deficient mice, while 11% in wild-type (Fig. 8B). Collectively, these results confirm that *NRF2* is an important factor for protecting renal tissue against CsA-induced EMT changes and fibrosis.

Discussion

Tissue fibrosis can result from inappropriate repair processes following tissue damage which can be caused by various stimuli, including infection, inflammation, and chemical stress [14]. Fibrosis accompanies the excessive deposition of extracellular matrix (ECM), leading to the destruction of tissues and eventual organ failure. Myofibroblasts play a central role in the process of fibrosis by producing ECM. EMT has been implicated as the primary mechanism of renal fibrogenesis through generation of mesenchymal type myofibroblasts from renal tubular epithelial cells [11–13]. Furthermore, Kim et al., have developed transgenic mice, in which lung epithelial cells were marked by β -galactosidase expression, and demonstrated that the increased pulmonary myofibroblasts in TGF β -treated transgenic mice were largely derived from lung epithelial cells through the EMT process [30]. These results indicate that the conversion of epithelial cells to myofibroblasts can be a common cellular/molecular mechanism of tissue fibrogenesis in various organs.

EMT requires the reprogramming of gene expression profiles, which can eventually lead to the disaggregation of epithelium, the loss of polarity and tight junctions, cytoskeletal rearrangements, and the production of ECM [9, 10]. Divergent paracrine and autocrine signals are known to induce this molecular reprogramming and, in particular, involvement of the TGF β -SMAD2/3 signaling in EMT has been well established. The critical role of TGF β in EMT has been confirmed by a study showing that targeted disruption of *SMAD3* in mice provided to a refractoriness to unilateral ureteral obstruction-induced renal interstitial fibrosis [31]. Conversely, overexpression of TGF β gene in mouse developed spontaneous intestinal fibrosis [32].

In addition to endogenous factors, chemical stress can be an important triggering factor for EMT. Changes in EMT markers have been detected in human tubular epithelial cells following CsA treatment [15, 29]. In our study, CsA treatment with concentration range of 1–8 μ M increased myofibroblast marker α -SMA in NRK-52E cells. With increasing concentration of CsA, changes in EMT markers were more prominent and the decrease in epithelial marker E-cadherin and the increase in vimentin and fibronectin-1 were accompanied. In particular, it was observed that Snail expression, which is one of transcription factors mediating EMT gene changes, was increased by CsA (Data not shown). Whilst, it was notable that CsA in NRK cells did not lead the elevation of TGF β expression unlike previous reports from animal studies showing the elevation of TGF β in CsA-treated kidneys. These observations suggest that CsA-mediated EMT may be associated with multiple mechanisms; changes in transcription factor activity, production of growth factors, and alterations in renal hormones appear to contribute to EMT changes through complicated physiological/cellular networks. In vitro observations could be confirmed in *vivo* evidence. We could identify the increase in α -SMA expression together with the decrease in E-cadherin in mouse kidney following CsA treatment for 3 weeks (data not shown). The underlying molecular mechanism of chemical-induced EMT has not been fully investigated, however increased production of TGF β has been suggested as an EMT-triggering factor in a CsA-induced animal fibrosis model [2]. In addition, the involvement of increased ROS generation in CsA-induced fibrosis can be envisioned. Accumulating lines of evidence support the concept that ROS affects EMT changes. In the context of the multifunctional role of ROS in cellular signaling pathways (e.g., MAPK/ERK and SMAD proteins) and transcription factors (e.g., AP-1 and HIF-1 α), elevated ROS might facilitate EMT process of epithelial cells and eventually, fibrosis [33, 34]. One example of this linkage of ROS to fibrosis is human idiopathic pulmonary fibrosis (IPF). At this time point, it has not been clearly demonstrated whether EMT is the major cause of IPF, however results showing cells expressing α -SMA were abundant in lung tissue from IPF patients support the association of EMT to IPF [35]. Patients with IPF have increased markers of oxidative stress and NAC has been the only therapeutic means to preserve lung function in these patients [36]. Furthermore, TGF β -mediated EMT changes could be inhibited by direct antioxidants such as NAC and catalase in rat renal tubular epithelial cells and alveolar epithelial cells [37, 38]. CsA is known to increase ROS levels in two ways: i) CsA treatment itself can reduce levels of components of the antioxidant defense system, thereby enhancing ROS levels in the kidney, and ii) CsA-mediated production of TGF β and angiotensin II can further enhance the level of ROS by activating NADPH oxidase [6, 7, 39]. These results imply that oxidative stress might be one of EMT-promoting factors in CsA-fibrosis model. Indeed, there have been several reports that antioxidant therapy could be beneficial in reducing the progression of renal fibrogenesis in CsA-treated patients [8, 40–42].

Our current results suggest that the NRF2 system, which orchestrates the expression of a wide array of antioxidant genes, plays a protective role against CsA-induced EMT-renal fibrosis. The NRF2 activator SFN treatment prevented EMT changes in rat tubular epithelial cells, whilst genetic inhibition of NRF2 in NRK cells aggravated CsA-induced EMT. Consistently, CsA-treatment in mice led to a higher burden of renal damage and fibrosis with increased expression of α -SMA and TGF β in *NRF2*-deficient mice compared to wild-type mice. A protective role of NRF2 against fibrosis has been demonstrated in several studies. Treatment of mice with bleomycin, which is an animal model for human pulmonary fibrosis, resulted in more severe lung fibrosis in *NRF2*-knockout mice compared to wild-type mice [43]. This report together with a recent finding that EMT can be detected in airways of bleomycin-treated *α -SMA-Cre* transgenic mice [44], indicate a modifying role of NRF2 in chemical-induced pulmonary fibrosis. Long-term treatment of *NRF2*-deficient mice with carbon tetrachloride strongly aggravated hepatic fibrosis compared to wild-type mice [45]. In accord with studies using genetic disruption of *NRF2*, treatment with

pharmacological activators of NRF2 signaling provides protection against fibrosis. In preclinical model of cystic fibrosis with mice carrying the R117H *CFTR* mutation, administration of synthetic triterpenoids significantly reduced airway inflammation in response to lipopolysaccharide [46]. Animals treated with ursodeoxycholic acid and coenzyme Q10 developed a lower degree of liver fibrosis, which was induced by bile duct ligation and dimethylnitrosamine treatment, respectively, through up-regulation of NRF2-target gene expression [47, 48]. Present study provides further evidence that the NRF2 pathway functions as a protective factor against chemical-induced renal fibrosis and suggests a novel role of the NRF2 system in modulating the EMT pathology.

In our rat tubular epithelial cell line system, CsA treatment in a concentration range from 2 to 8 μ M did not alter cellular redox conditions with regard to the levels of GSH/GSSG. While it was notable that HO-1 expression could be strongly induced by CsA and this induction was NRF2-dependent. Although we could not detect significant activation of ARE-reporter gene expression as well as other typical ARE-regulated genes such as GCL and NQO1, it was found that nuclear NRF2 level was marginally increased and GCLM expression was slightly enhanced by CsA. These results raise a possibility that CsA alters the NRF2 system in a small degree and HO-1 expression in NRK cells might be relatively more sensitive to NRF2 than other target genes such as GCLC. It can be also possible that second transcription factors might be controlling HO-1 expression by CsA. For instance, CsA treatment increased AP-1 transcription activity in NRK cells, implying NRF2-dependent transcription factors may lead to HO-1 induction in an indirect way. Pharmacological activation and genetic inhibition studies confirmed the protective role of HO-1 in CsA-mediated EMT gene changes. Other studies indicate that HO-1 induction exerts renal protective effects in various animal models with ischemia renal failure, radiation-induced nephropathy, and cisplatin nephrotoxicity [24, 49]. In particular, a role of HO-1 in renal fibrosis has been suggested by two independent studies. Hemin treatment, which is an inducer of HO-1 expression, decreased renal levels of TGF β and in turn suppressed tubulointerstitial fibrosis in rat unilateral ureteral obstruction model [50]. By contrast, *HO-1* deficiency in mice facilitated renal fibrosis and enhanced α -SMA expression compared to wild-type animals in this fibrosis model [51]. However, as NRF2 regulates a broad-based expression of antioxidant genes, the protective effects of NRF2 shown in animals might be accounted by the integrated overall contributions of various NRF2-target genes, which can affect the cell signaling pathways and transcription factor activity associated with the EMT-fibrosis process.

Collectively, the results of the present study provide the evidence demonstrating that the NRF2 system plays a protective role in CsA-mediated renal fibrosis. The beneficial effect of NRF2 on CsA toxicity could be accounted by the inhibitory function of NRF2 in CsA-mediated EMT gene changes, and among NRF2-target genes, HO-1 might have a major contribution to prevent EMT. Since a growing body of evidence indicates that EMT is a cellular/molecular mechanism of fibrogenesis of multiple organs, identification of factors that regulate the EMT process will render valuable information to control EMT and further the development of anti-fibrogenic agents. Therefore, the use of small molecule NRF2-specific activators might be a potential strategy to prevent or attenuate EMT-fibrosis process evoked by divergent stresses.

Acknowledgments

We thank to Patrick M. Dolan (Johns Hopkin University, Baltimore, MD, USA) for maintaining and genotyping mice. This work was supported by National Research Foundation of Korea Grant funded by the Korean Government (2009-0066689) to M-K Kwak and NIH grant CA94076 to T.W. Kensler.

Abbreviations

GSH	glutathione
GCLC	catalytic subunit of γ -glutamylcysteine ligase
GCLM	modulatory subunit of γ -glutamylcysteine ligase
HO-1	heme oxygenase-1
GR	glutathione reductase
GSTs	glutathione <i>S</i> -transferases
NQO1, NAD(P)H	quinone oxidoreductase-1
ROS	reactive oxygen species
DTNB	5,5-dithiobis (2-nitrobenzoic acid)
MTT	3-(4,5-dimethylthiazol-2-yl)-2,5-diphenyltetrazolium bromide
ARE	antioxidant response element
α-SMA	α -smooth muscle actin
CsA	cyclosporine A
SFN	sulforaphane
HPRT	hypoxanthine-guanine phosphoribosyltransferase
EMT	epithelial-mesenchymal transition
TGFβ	transforming growth factor- β
ECM	extracellular matrix
NAC	N-acetylcysteine
Fn-1	fibronectin-1
CoPP	cobalt protoporphyrin
DMSO	dimethylsulfoxide

References

1. Grinyo JM, Cruzado JM. Cyclosporine nephrotoxicity. *Transplant Proc.* 2004; 36:240S–242S. [PubMed: 15041345]
2. Vitko S, Viklicky O. Cyclosporine renal dysfunction. *Transplant Proc.* 2004; 36:243S–247S. [PubMed: 15041346]
3. Bennett WM, DeMattos A, Meyer MM, Andoh T, Barry JM. Chronic cyclosporine nephropathy: the Achilles' heel of immunosuppressive therapy. *Kidney Int.* 1996; 50: 1089–1100. [PubMed: 8887265]
4. Oriji GK, Keiser HR. Role of nitric oxide in cyclosporine A-induced hypertension. *Hypertension.* 1998; 32: 849–855. [PubMed: 9822443]
5. Remuzzi G, Perico N. Cyclosporine-induced renal dysfunction in experimental animals and humans. *Kidney Int Suppl.* 1995; 52:S70–74. [PubMed: 8587288]
6. Buetler TM, Cottet-Maire F, Krauskopf A, Ruegg UT. Does cyclosporin A generate free radicals? *Trends Pharmacol Sci.* 2000; 21:288–290. [PubMed: 10918629]
7. Jimenez R, Galan AI, Gonzalez de Buitrago JM, Palomero J, Munoz ME. Glutathione metabolism in cyclosporine A-treated rats: dose- and time-related changes in liver and kidney. *Clin Exp Pharmacol Physiol.* 2000; 27: 991–996. [PubMed: 11117236]

8. Wang C, Salahudeen AK. Lipid peroxidation accompanies cyclosporine nephrotoxicity: effects of vitamin E. *Kidney Int.* 1995; 47:927–934. [PubMed: 7752594]
9. Kalluri R, Weinberg RA. The basics of epithelial-mesenchymal transition. *J Clin Invest.* 2009; 119: 1420–1428. [PubMed: 19487818]
10. Lee JM, Dedhar S, Kalluri R, Thompson EW. The epithelial-mesenchymal transition: new insights in signaling, development, and disease. *J Cell Biol.* 2006; 172:973–981. [PubMed: 16567498]
11. Radisky DC, Kenny PA, Bissell MJ. Fibrosis and cancer: do myofibroblasts come also from epithelial cells via EMT? *J Cell Biochem.* 2007; 101: 830–839. [PubMed: 17211838]
12. Iwano M, Plieth D, Danoff TM, Xue C, Okada H, Neilson EG. Evidence that fibroblasts derive from epithelium during tissue fibrosis. *J Clin Invest.* 2002; 110:341–350. [PubMed: 12163453]
13. Kalluri R, Neilson EG. Epithelial-mesenchymal transition and its implications for fibrosis. *J Clin Invest.* 2003; 112: 1776–1784. [PubMed: 14679171]
14. Wynn TA. Cellular and molecular mechanisms of fibrosis. *J Pathol.* 2008; 214:199–210. [PubMed: 18161745]
15. Slattery C, Campbell E, McMorrow T, Ryan MP. Cyclosporine A-induced renal fibrosis: a role for epithelial-mesenchymal transition. *Am J Pathol.* 2005; 167:395–407. [PubMed: 16049326]
16. Kobayashi M, Yamamoto M. Molecular mechanisms activating the Nrf2-Keap1 pathway of antioxidant gene regulation. *Antioxid Redox Signal.* 2005; 7: 385–394. [PubMed: 15706085]
17. Kwak MK, Wakabayashi N, Greenlaw JL, Yamamoto M, Kensler TW. Antioxidants enhance mammalian proteasome expression through the Keap1-Nrf2 signaling pathway. *Mol Cell Biol.* 2003; 23: 8786–8794. [PubMed: 14612418]
18. Li W, Kong AN. Molecular mechanisms of Nrf2-mediated antioxidant response. *Mol Carcinog.* 2009; 48:91–104. [PubMed: 18618599]
19. Tong KI, Kobayashi A, Katsuoka F, Yamamoto M. Two-site substrate recognition model for the Keap1-Nrf2 system: a hinge and latch mechanism. *Biol Chem.* 2006; 387: 1311–1320. [PubMed: 17081101]
20. Cho HY, Kleeberger SR. Nrf2 protects against airway disorders. *Toxicol Appl Pharmacol.* 10.1016/j.taap.2009.07.024
21. Johnson JA, Johnson DA, Kraft AD, Calkins MJ, Jakel RJ, Vargas MR, Chen PC. The Nrf2-ARE pathway: an indicator and modulator of oxidative stress in neurodegeneration. *Ann N Y Acad Sci.* 2008; 1147: 61–69. [PubMed: 19076431]
22. Kwak MK, Kensler TW. Targeting NRF2 Signaling for Cancer Chemoprevention. *Toxicol Appl Pharmacol.* 2009 In press.
23. Osburn WO, Yates MS, Dolan PD, Chen S, Liby KT, Sporn MB, Taguchi K, Yamamoto M, Kensler TW. Genetic or pharmacologic amplification of nrf2 signaling inhibits acute inflammatory liver injury in mice. *Toxicol Sci.* 2008; 104:218–227. [PubMed: 18417483]
24. Abraham NG, Kappas A. Pharmacological and clinical aspects of heme oxygenase. *Pharmacol Rev.* 2008; 60: 79–127. [PubMed: 18323402]
25. Griffith OW. Determination of glutathione and glutathione disulfide using glutathione reductase and 2-vinylpyridine. *Anal Biochem.* 1980; 106: 207–212. [PubMed: 7416462]
26. Shim G-S, Manandhar S, Shin D-H, Kim T-H, Kwak M-K. Acquisition of doxorubicin resistance in ovarian carcinoma cells accompanies activation of the NRF2-GSH pathway. *Free Radic Biol Med.* 2009; 47: 1619–1631. [PubMed: 19751820]
27. Itoh K, Chiba T, Takahashi S, Ishii T, Igarashi K, Katoh Y, Oyake T, Hayashi N, Satoh K, Hatayama I, Yamamoto M, Nabeshima Y. An Nrf2/small Maf heterodimer mediates the induction of phase II detoxifying enzyme genes through antioxidant response elements. *Biochem Biophys Res Commun.* 1997; 236:313–322. [PubMed: 9240432]
28. Park HM, Cho JM, Lee HR, Shim GS, Kwak MK. Renal protection by 3H-1,2-dithiole-3-thione against cisplatin through the Nrf2-antioxidant pathway. *Biochem Pharmacol.* 2008; 76:597–607. [PubMed: 18656455]
29. McMorrow T, Gaffney MM, Slattery C, Campbell E, Ryan MP. Cyclosporine A induced epithelial-mesenchymal transition in human renal proximal tubular epithelial cells. *Nephrol Dial Transplant.* 2005; 20: 2215–2225. [PubMed: 16030052]

30. Kim KK, Kugler MC, Wolters PJ, Robillard L, Galvez MG, Brumwell AN, Sheppard D, Chapman HA. Alveolar epithelial cell mesenchymal transition develops in vivo during pulmonary fibrosis and is regulated by the extracellular matrix. *Proc Natl Acad Sci U S A*. 2006; 103: 13180–13185. [PubMed: 16924102]
31. Sato M, Muragaki Y, Saika S, Roberts AB, Ooshima A. Targeted disruption of TGF-beta1/Smad3 signaling protects against renal tubulointerstitial fibrosis induced by unilateral ureteral obstruction. *J Clin Invest*. 2003; 112: 1486–1494. [PubMed: 14617750]
32. Vallance BA, Gunawan MI, Hewlett B, Bercik P, Van Kampen C, Galeazzi F, Sime PJ, Gauldie J, Collins SM. TGF-beta1 gene transfer to the mouse colon leads to intestinal fibrosis. *Am J Physiol Gastrointest Liver Physiol*. 2005; 289:G116–128. [PubMed: 15778431]
33. Adler V, Yin Z, Tew KD, Ronai Z. Role of redox potential and reactive oxygen species in stress signaling. *Oncogene*. 1999; 18: 6104–6111. [PubMed: 10557101]
34. Kinnula VL, Myllarniemi M. Oxidant-antioxidant imbalance as a potential contributor to the progression of human pulmonary fibrosis. *Antioxid Redox Signal*. 2008; 10:727–738. [PubMed: 18177235]
35. Willis BC, Liebler JM, Luby-Phelps K, Nicholson AG, Crandall ED, du Bois RM, Borok Z. Induction of epithelial-mesenchymal transition in alveolar epithelial cells by transforming growth factor-beta1: potential role in idiopathic pulmonary fibrosis. *Am J Pathol*. 2005; 166: 1321–1332. [PubMed: 15855634]
36. Demedts M, Behr J, Buhl R, Costabel U, Dekhuijzen R, Jansen HM, MacNee W, Thomeer M, Wallaert B, Laurent F, Nicholson AG, Verbeken EK, Verschakelen J, Flower CD, Capron F, Petruzzelli S, De Vuyst P, van den Bosch JM, Rodriguez-Becerra E, Corvasce G, Lankhorst I, Sardina M, Montanari M. High-dose acetylcysteine in idiopathic pulmonary fibrosis. *N Engl J Med*. 2005; 353: 2229–2242. [PubMed: 16306520]
37. Felton VM, Borok Z, Willis BC. N-acetylcysteine Inhibits Alveolar Epithelial-Mesenchymal Transition. *Am J Physiol Lung Cell Mol Physiol*. 2009
38. Rhyu DY, Yang Y, Ha H, Lee GT, Song JS, Uh ST, Lee HB. Role of reactive oxygen species in TGF-beta1-induced mitogen-activated protein kinase activation and epithelial-mesenchymal transition in renal tubular epithelial cells. *J Am Soc Nephrol*. 2005; 16: 667–675. [PubMed: 15677311]
39. Djamali A, Vidyasagar A, Adulla M, Hullett D, Reese S. Nox-2 is a modulator of fibrogenesis in kidney allografts. *Am J Transplant*. 2009; 9: 74–82. [PubMed: 18976289]
40. Galletti P, Di Gennaro CI, Migliardi V, Indaco S, Della Ragione F, Manna C, Chiodini P, Capasso G, Zappia V. Diverse effects of natural antioxidants on cyclosporin cytotoxicity in rat renal tubular cells. *Nephrol Dial Transplant*. 2005; 20:1551–1558. [PubMed: 15855205]
41. Parra Cid T, Conejo Garcia JR, Carballo Alvarez F, de Arriba G. Antioxidant nutrients protect against cyclosporine A nephrotoxicity. *Toxicology*. 2003; 189:99–111. [PubMed: 12821286]
42. Zhong Z, Connor HD, Yin M, Moss N, Mason RP, Bunzendahl H, Forman DT, Thurman RG. Dietary glycine and renal denervation prevents cyclosporin A-induced hydroxyl radical production in rat kidney. *Mol Pharmacol*. 1999; 56: 455–463. [PubMed: 10462532]
43. Cho HY, Reddy SP, Yamamoto M, Kleeberger SR. The transcription factor NRF2 protects against pulmonary fibrosis. *Faseb J*. 2004; 18:1258–1260. [PubMed: 15208274]
44. Wu Z, Yang L, Cai L, Zhang M, Cheng X, Yang X, Xu J. Detection of epithelial to mesenchymal transition in airways of a bleomycin induced pulmonary fibrosis model derived from an alpha-smooth muscle actin-Cre transgenic mouse. *Respir Res*. 2007; 8:1. [PubMed: 17207287]
45. Xu W, Hellerbrand C, Kohler UA, Bugnon P, Kan YW, Werner S, Beyer TA. The Nrf2 transcription factor protects from toxin-induced liver injury and fibrosis. *Lab Invest*. 2008; 88: 1068–1078. [PubMed: 18679376]
46. Nichols DP, Ziady AG, Shank SL, Eastman JF, Davis PB. The Triterpenoid CDDO Limits Inflammation in Preclinical Models of Cystic Fibrosis Lung Disease. *Am J Physiol Lung Cell Mol Physiol*. 2009
47. Choi HK, Pokharel YR, Lim SC, Han HK, Ryu CS, Kim SK, Kwak MK, Kang KW. Inhibition of liver fibrosis by solubilized coenzyme Q10: Role of Nrf2 activation in inhibiting transforming growth factor-beta1 expression. *Toxicol Appl Pharmacol*. 2009

48. Yang H, Ramani K, Xia M, Ko KS, Li TW, Oh P, Li J, Lu SC. Dysregulation of glutathione synthesis during cholestasis in mice: molecular mechanisms and therapeutic implications. *Hepatology*. 2009; 49: 1982–1991. [PubMed: 19399914]
49. Abraham NG, Cao J, Sacerdoti D, Li X, Drummond GS. Heme Oxygenase: The Key to Renal Function Regulation. *Am J Physiol Renal Physiol*. 2009
50. Kim JH, Yang JI, Jung MH, Hwa JS, Kang KR, Park DJ, Roh GS, Cho GJ, Choi WS, Chang SH. Heme oxygenase-1 protects rat kidney from ureteral obstruction via an antiapoptotic pathway. *J Am Soc Nephrol*. 2006; 17:1373–1381. [PubMed: 16597687]
51. Kie JH, Kapturczak MH, Traylor A, Agarwal A, Hill-Kapturczak N. Heme oxygenase-1 deficiency promotes epithelial-mesenchymal transition and renal fibrosis. *J Am Soc Nephrol*. 2008; 19:1681–1691. [PubMed: 18495963]

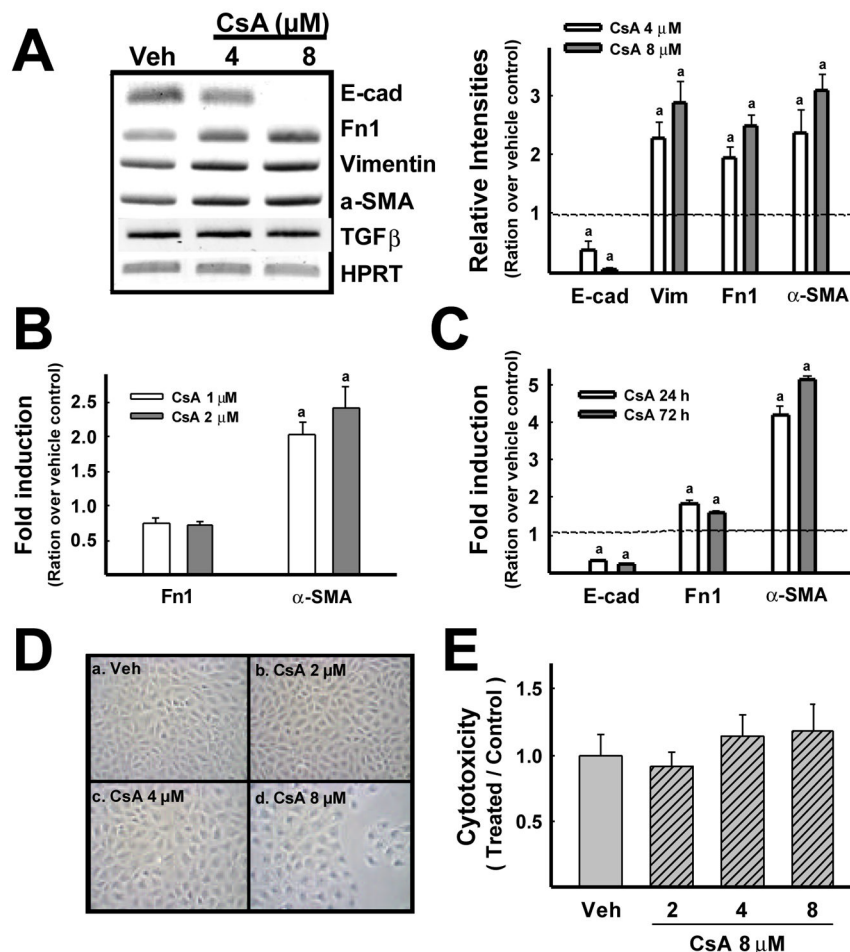


Fig 1. Effect of CsA on changes in EMT markers in rat tubular epithelial NRK cells. (A) Transcript levels of E-cadherin (E-cad), fibronectin-1 (Fn-1), vimentin, α -SMA, TGF β , and HPRT were measured using a RT-PCR analysis following treatment of NRK cells with vehicle (Veh, ethanol) or CsA (4 and 8 μ M) for 48 h. Relative intensities were obtained following normalization of each gene expression by levels of HPRT. Values are means \pm S.E. from three experiments. (B) Transcript levels for Fn-1, α -SMA and HPRT were measured using real-time PCR analysis following with vehicle (Veh) or low concentrations of CsA (1 and 2 μ M) for 48 h. Fold inductions are ratios over vehicle control following normalization of each gene expression by levels of HPRT. Values are means \pm S.E. from three experiments. (C) Transcript levels of E-cad, Fn-1, α -SMA and HPRT were measured using real-time PCR analysis following with vehicle (Veh) or 8 μ M CsA for 24 h or 72 h. Fold inductions are ratios over vehicle control following normalization of each gene expression by levels of HPRT. Values are means \pm S.E. from three experiments. ^aP<0.05 compared with vehicle-treated cells. (D) Morphological changes of NRK cells following treatment with vehicle (Veh) or CsA (2, 4, and 8 μ M) for 48 h. (E) Cytotoxicity by CsA was monitored using bis-AAF-R110 substrate (Promega) and measuring fluorescent intensities following treatment with vehicle (Veh) or CsA (2, 4, and 8 μ M) for 48 h. Values are means \pm S.E. from eight experiments.

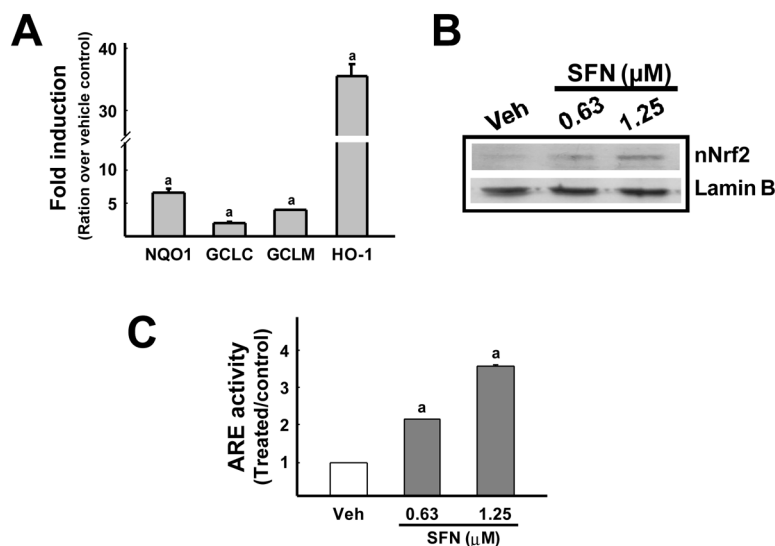


Fig 2. Effect of SFN on NRF2 activity in NRK cells. (A) Transcript levels of NRF2-target genes (NQO1, GCLC, and GCLM) and HPRT were measured using real-time PCR analysis following treatment of NRK cells with vehicle (Veh) or 1.25 μM SFN for 24 h. Level of HO-1 transcripts was assessed 6 h after treatment with SFN. Fold inductions are ratios over vehicle control following normalization by HPRT levels. Values are means \pm S.E. from three experiments. ^a $P < 0.05$ compared with vehicle-treated cells. (B) Nuclear levels of NRF2 protein and lamin B were determined by immunoblot analysis following treatment with vehicle (Veh) or SFN (0.63 or 1.25 μM) for 6 h. (C) ARE-driven luciferase activities following treatment with CsA. NRK cells were transfected with the luciferase reporter plasmid containing the *NQO1 ARE* and were treated with vehicle (Veh) or SFN (0.63 or 1.25 μM) for 24 h. Measurement of luciferase activities was performed by the Dual Luciferase System using the Renilla luciferase control plasmid. Values are means \pm S.E. from four experiments. ^a $P < 0.05$ compared with vehicle-treated control cells.

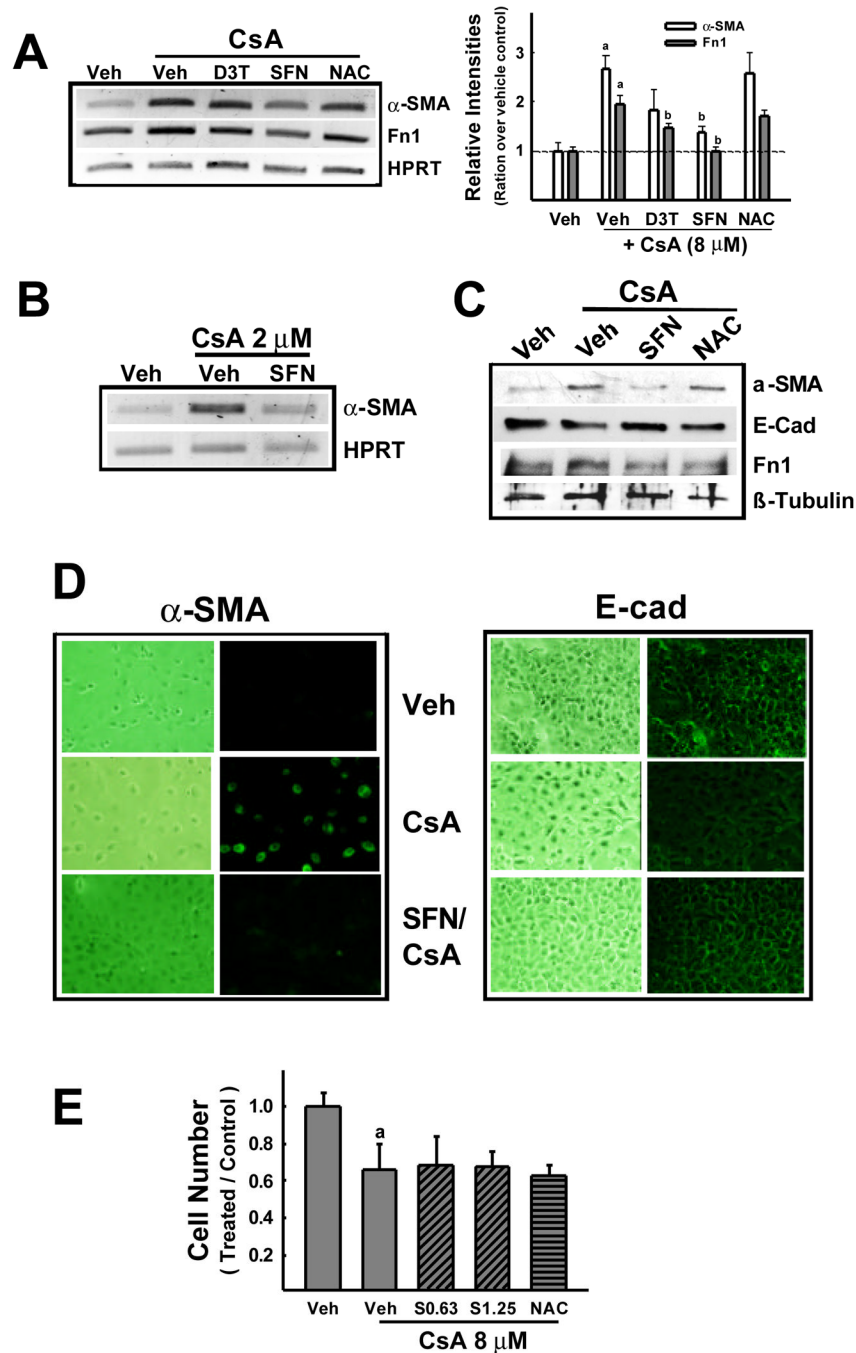


Fig 3. Protective effect of SFN against CsA-induced EMT gene changes in NRK cells. (A) Transcript levels for α -SMA, Fn-1 and HPRT were measured using RT-PCR analyses. Cells were pre-treated with vehicle (Veh, DMSO), D3T (5 μ M), SFN (1.25 μ M) or NAC (5 mM) for 24 h and followed by addition of vehicle (Veh, ethanol) or 8 μ M CsA for a further incubation for 48 h. Relative intensities were obtained as ratios over vehicle control following normalization by HPRT levels. Values are means \pm S.E. from three experiments. (B) Transcript level for α -SMA and HPRT were measured following low concentration of CsA (2 μ M) with or without SFN pre-incubation. (C) Protein levels for α -SMA, E-cad, Fn-1

and β -tubulin were determined by using an immunoblot analysis. Cells were pre-incubated with vehicle (Veh, DMSO), SFN (1.25 μ M) or NAC (5 mM) for 24 h and the addition of vehicle (ethanol) or CsA (8 μ M) was followed. After the completion of drug treatment, total cellular lysates were prepared for immunoblot analyses. (D) Immunocytochemical staining of α -SMA and E-cad in NRK cells following CsA and SFN treatment. Cells were pre-treated with vehicle (Veh, DMSO) or 1.25 μ M SFN for 24 h and followed by incubation with CsA (8 μ M). At least three similar staining were obtained. (E) Cell numbers were monitored by MTT analyses following pre-incubation of NRK cells with vehicle (Veh), SFN (0.63 or 1.25 μ M) or NAC (5 mM) for 24 h, followed by 8 μ M CsA incubation for 48 h.

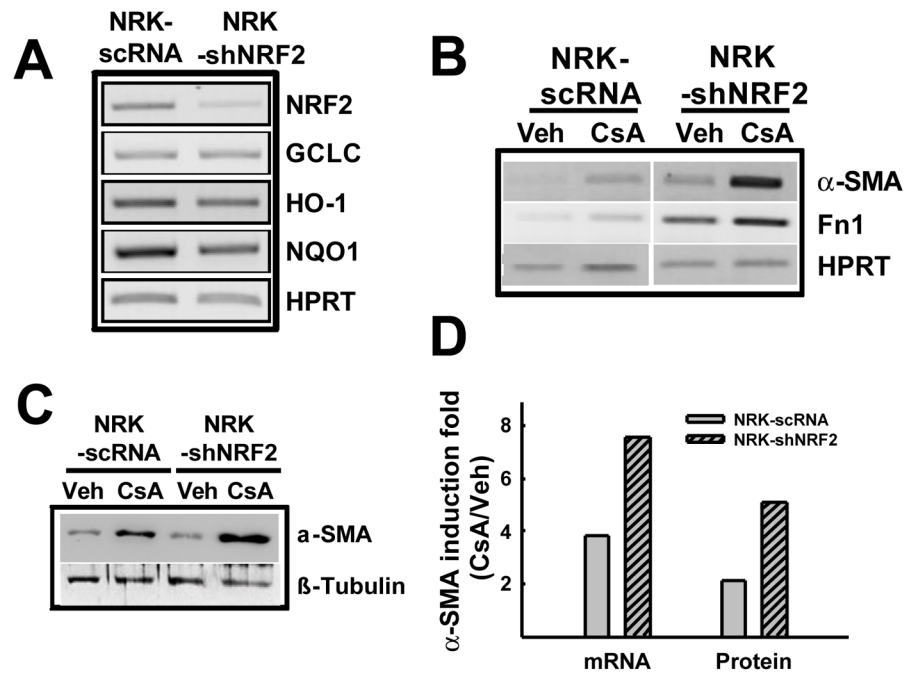
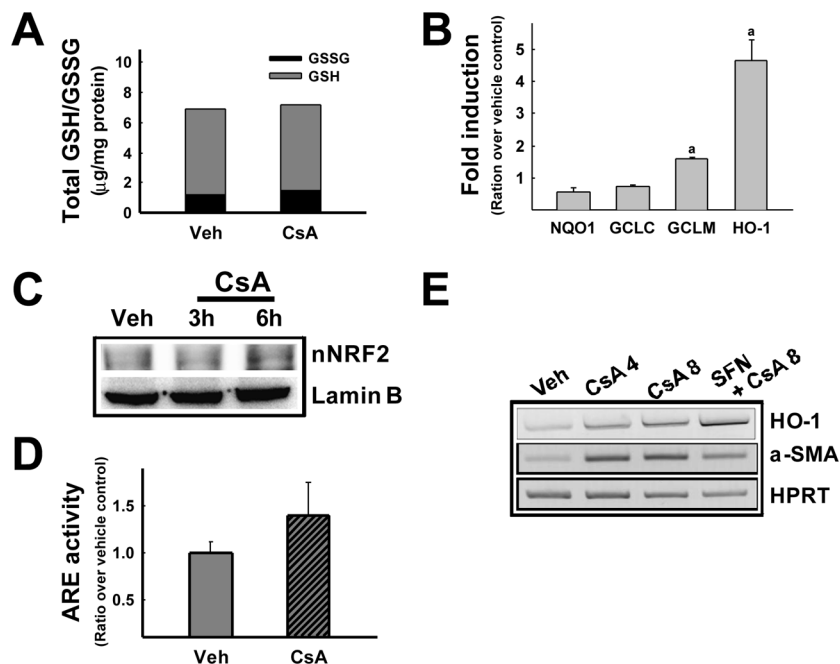


Fig 4. CsA-induced α -SMA expression was affected by NRF2 levels. (A) Establishment of NRF2-inhibited NRK cells by using the lentiviral delivery system. Cells were transduced with lentiviral particles containing either a nonspecific scRNA-expressing viral plasmid or NRF2-targeting shRNA-expressing plasmid, followed by selection with puromycin. Stable cell lines expressing scRNA (NRK-scRNA) or NRF2 shRNA (NRK-shNRF2) were obtained and transcript levels of NRF2, GCLC, HO-1, NQO1 and HPRT were determined by RT-PCR analyses. (B, D) EMT gene change in NRF2-inhibited cells. NRK-scRNA and NRK-shNRF2 cells were incubated with vehicle (Veh, ethanol) or 8 μ M CsA for 48 h and transcript levels for α -SMA, Fn-1 and HPRT were monitored by RT-PCR analyses. (C, D) Inducible levels of α -SMA in NRK-scRNA and NRK-shNRF2 cells. Protein levels for α -SMA and β -tubulin were measured using immunoblot analyses. Relative α -SMA levels were determined following normalization of transcript and protein levels by HPRT and β -tubulin levels, respectively.

**Fig 5.**

Effect of CsA on the NRF2 system in NRK cells. (A) Total cellular GSH and oxidized GSH (GSSG) levels following treatment with CsA. Cells were incubated with vehicle (Veh) or 8 μ M CsA for 48 h and total GSH content was measured using the kinetic enzymatic recycling assay system based on the oxidation of GSH by DTNB. Oxidized GSH levels were determined by incubating cells with 2-vinylpyridine (10 μ M) for 1 h. Values are means \pm S.E. from five experiments. (B) Transcript levels for NRF2-target genes (GCLC, GCLM, NQO1 and HO-1) and HPRT were measured using a real-time PCR analysis following treatment of NRK cells with vehicle (Veh, ethanol) or 8 μ M CsA for 48 h. Fold inductions are ratios over vehicle control following normalization by HPRT levels. Values are means \pm S.E. from three experiments. ^aP<0.05 compared with vehicle-treated cells. (C) Nuclear NRF2 protein level was assessed by immunoblot analysis following CsA (8 μ M) incubation for 3 h and 6 h. (D) ARE-driven luciferase activities following CsA treatment. NRK cells were transfected with the ARE-containing reporter plasmid and were incubated with vehicle (Veh) or 8 μ M CsA for 48 h. Dual luciferase activities were monitored and Firefly luciferase levels were normalized by Renilla luciferase levels. Values are means \pm S.E. from three experiments. (E) Transcript levels of HO-1, α -SMA and HPRT following CsA and SFN treatment. Cells were pre-incubated with vehicle (Veh) or 1.25 μ M SFN for 18 h and CsA incubation was followed for 48 h.

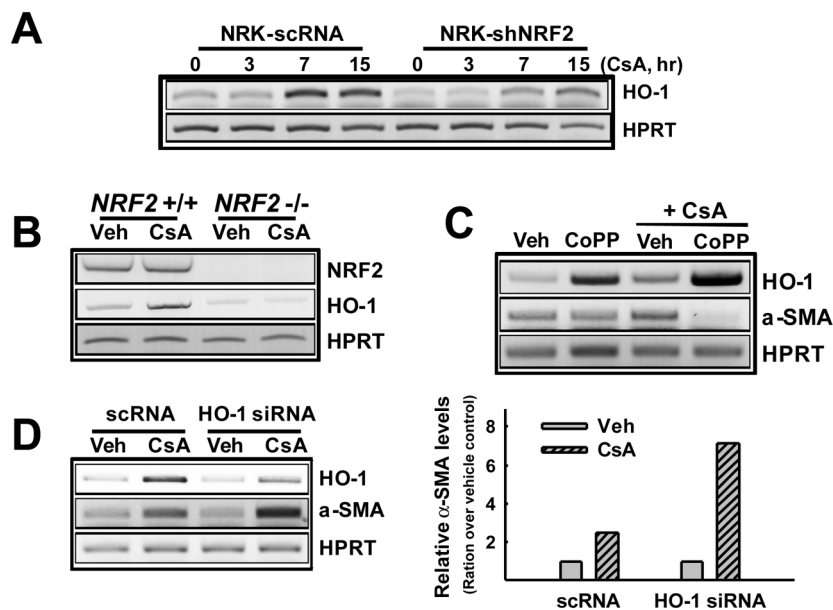


Fig 6. HO-1 involvement in NRF2-mediated protection against CsA-induced EMT. (A) HO-1 inducibility in NRF2-inhibited NRK cells. Transcript levels of HO-1 and HPRT were determined following incubation of NRK-scRNA or NRK-shNRF2 cells with vehicle (ethanol) for 3 h or 8 μ M CsA for 3, 7, or 15 h. (B) CsA-induced HO-1 expression in MEFs from wild-type (*NRF2*^{+/+}) or *NRF2*-deficient mice (*NRF2*^{-/-}). Transcript levels of NRF2, HO-1 and HPRT were measured following incubation of MEFs with vehicle (Veh) or CsA (8 μ M) for 48 h. (C) Effect of HO-1 inducer CoPP on CsA-induced α -SMA expression. CoPP (100 μ M) was pre-incubated for 24 h and followed by CsA (8 μ M) incubation. Transcript levels for HO-1, α -SMA and HPRT were determined by RT-PCR analyses. (D) CsA-induced α -SMA expression in HO-1 siRNA transfected cells. Nonspecific scRNA or HO-1 targeting siRNA were transfected into NRK cells and CsA-induced α -SMA expression was determined.

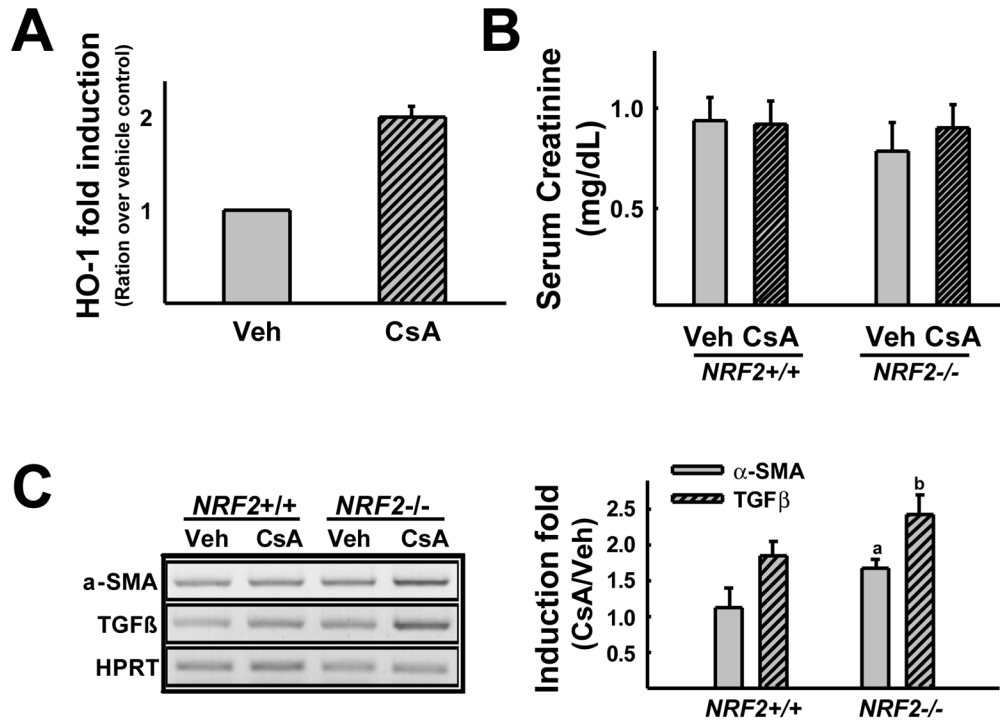


Fig 7. Enhanced expression of EMT markers following CsA treatment in *NRF2*-deficient mice. (A) HO-1 induction by CsA in mouse kidneys. ICR wild-type mice were treated with vehicle (olive oil) or CsA (30 mg/kg, *p.o.*) for two consecutive days and renal HO-1 level was monitored by real-time PCR analysis. Fold inductions are ratios over vehicle control following normalization of HO-1 expression by HPRT levels. Values are means ± S.E. from three experiments. ^a*P*<0.05 compared with vehicle-treated cells. (B) Renal function assessment in mice following CsA treatment for 2 weeks. Wild-type (*NRF2*^{+/+}) and *NRF2*-deficient (*NRF2*^{-/-}) mice were treated with vehicle (Veh, olive oil) or CsA (30 mg/kg) by *gavage* once a day for 2 weeks. Blood was collected and levels of serum creatinine were monitored. Values are means ± SE from 3 individual animals. (C) Transcript levels for α-SMA, TGFβ, and HPRT in the kidney of wild-type (*NRF2*^{+/+}) and *NRF2*-deficient (*NRF2*^{-/-}) mice treated with vehicle (Veh, olive oil) or CsA. Relative intensities were obtained following normalization of expression levels of each gene by HPRT levels. Values are means ± S.E. from 3 individual animals. ^a*P* < 0.01 compared with wild-type (*NRF2*^{+/+}). ^b*P* < 0.01 compared with *NRF2*-deficient mice (*NRF2*^{-/-}).

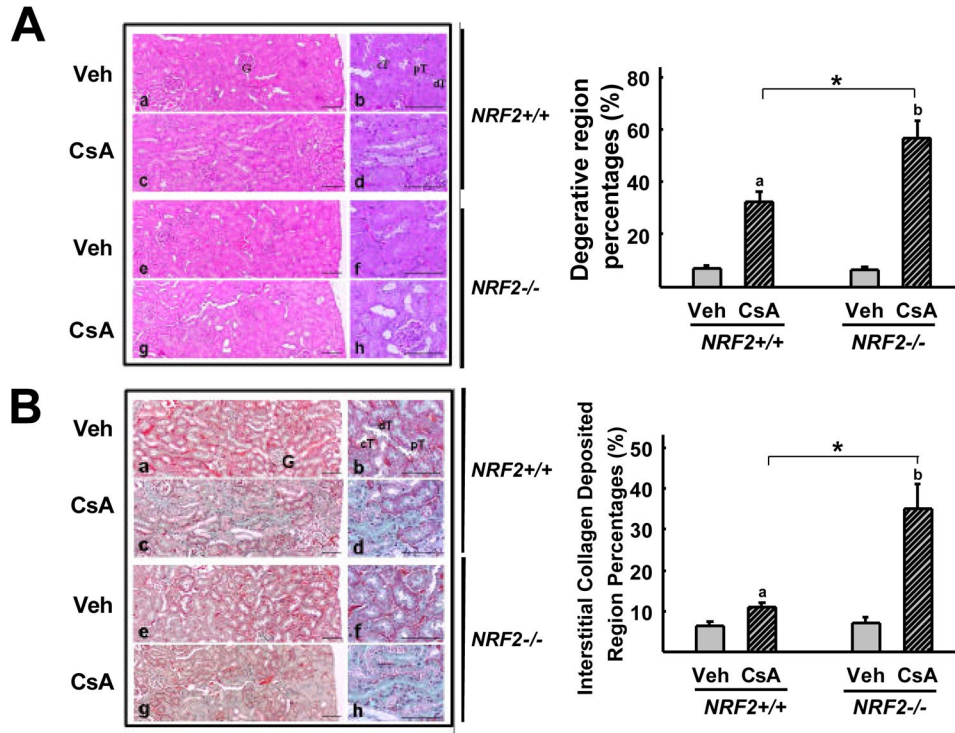


Fig 8. Enhanced CsA-renal fibrosis in *NRF2*-deficient mice. (A) Histopathological changes of the kidney from CsA-treated mice. Histological profiles were detected by H&E staining in wild-type (*NRF2*^{+/+}) mice treated with vehicle (a, b) or CsA (c, d) and in *NRF2*-deficient (*NRF2*^{-/-}) mice treated with vehicle (e, f) or CsA (g, h). Focal tubular necrosis, degeneration, and thickening of basement membrane were observed in CsA-treated mice. Different magnifications of histology are shown in each treatment group. Degenerative region percentages were obtained in 1 mm² fields of each kidney. Two fields were selected randomly in each kidney sample. (B) Collagen deposition profiles in wild-type (*NRF2*^{+/+}) vehicle control (a, b), wild-type CsA group (c, d), *NRF2*-deficient (*NRF2*^{-/-}) vehicle control (e, f), and *NRF2*-deficient CsA group (g, h). Collagen is shown in green color following the Masson's trichrome staining. Values are means ± S.E. of six histological fields (two fields in each kidney sample). ^a, P < 0.01 compared with wild-type (*NRF2*^{+/+}) vehicle control. ^b, P < 0.01 compared with *NRF2*-deficient mice (*NRF2*^{-/-}) vehicle control. *, P < 0.01 compared with CsA-treated wild-type mice. G, glomeruli; pT, proximal convoluted tubule; dT, distal convoluted tubule; cT, collecting duct; Scale bar = 80 μm.